Miniaturized and Highly Efficient Substrate Integrated Waveguide (SIW) Cavity Slot Antenna at 28GHz Based on Through Fused-Silica Via (TFS) Technology

Hanna Jang
Electrical and Computer Engineering
University of Florida
Gainesville, FL, USA
hannajang@ufl.edu

Payman Pahlavan

Electrical and Computer Engineering
University of Florida
Gainesville, FL, USA
paymanpahlavan@ufl.edu

Yong-Kyu Yoon
Electrical and Computer Engineering
University of Florida
Gainesville, FL, USA
ykyoon@ece.ufl.edu

Abstract— A miniaturized high-efficiency cavity meander-slot antenna, utilizing Substrate Integrated Waveguide (SIW) and Through Fused-Silica Via (TFV) technologies, is designed for operation at 28GHz for millimeter-wave (mmWave) applications. The SIW cavity antenna, with an electrical size of $1.92 \times 1.92 \ mm^2$ $(0.032 \lambda_0^2)$, achieves a 44% reduction in area compared to a conventional patch antenna. Noteworthy attributes of the TFVwall structure include: 1) An electromagnetic shielding effect that significantly suppresses mutual coupling in array antennas with a distance (edge-to-edge) of 0.14 mm (0.026 λ_a), 2) a compact footprint with enhanced antenna performance, and 3) adjustable impedance matching through manipulation of the via parameters. . The impact of via diameter pitch on the resonance frequency and return loss has been investigated. The proposed antenna obtains a peak gain of 5.91 dB, a radiation efficiency of 88%, with the isolation enhanced by 17.03 dB.

Keywords—Miniaturized antennas, slotted patch antenna, substrate integrated waveguide (SIW) antenna, mutual coupling reduction, heterogeneous integration, antenna-in-package.

I. INTRODUCTION

Recently the mobile network has encountered severe data spectrum traffic on the cellular network system in worldwide due to the necessary role of wireless mobile electronics on smartphones, tablet and wearable devices in the daily life. This surge in mobile system demand requires high data rate speed, increased bandwidth and low data latency toward 5G mobile communication in the millimeter wave (mmWave) bands [1]. Mm-wave technology not only offers a wide bandwidth that enables higher data transmission and broad network capability, but also brings about smaller and more light-weight device [2].

As the fundamental part of wireless communication, the gain and adaptive beamforming capabilities of array antennas enable Gbps data rates in mmWave systems [3]. Patch antenna, widely chosen due to its low-profile, cost-effectiveness, and ease of fabrication, often features array configurations to improve gain and efficiency. However, this array configuration occupies a substantial footprint beyond the limited package size of small wireless devices.

Various approaches for achieving antenna miniaturization for antenna-in-packaging solutions have been reported, such as loading capacitors and inductors [4], and shorting pins for operating in half-mode [5], [6]. However, these methods are associated with a decrease in the gain and overall efficiency of the antenna. Employing a high permittivity substrate a wellestablished approach to reduce the size of the patch antenna. However, this leads to a reduction in both bandwidth and radiation efficiency due to increased surface wave excitation. In recent years, artificial metamaterial structures have been employed to reduce the footprint of the patch antenna. Composite right/left-handed (CRLH) mushroom structure based circularly polarized (CP) patch antenna [7] and complementary split-ring resonator (CSRR) loaded wide-beamwidth CP antenna [8] has been introduced for the purpose of miniaturization. Defected ground structure (DGS) [9] could also be used to achieve miniaturization, resulting in design complexity. In [9], a reduction in patch size by 68% was reported through the application of a Minkowski fractal DGS. Additionally, the size of the patch antenna can be minimized by employing a coupled slot patch [10], [11]. In [10], an area reduction of 60% is reported, and in [11], the size of the antenna decreased by 90.6%, with a significant decrease in antenna efficiency.

In this work, we present the Through Fused-Silica Via (TFV) based compact SIW meander-slot cavity antenna on dual-layer fused silica substrates operating at 28GHz. The meander-slot is effective in reducing the dimensions of antennas and mutual coupling between antenna elements in 2x2 arrays [12,13]. The novel TFV-based antenna with meander-slot loading features a simple integrated structure, low-loss, and a small footprint, making it suitable for applications in 5G communications and advanced 3D packaging systems. Using a low-loss fused-silica substrate with a dielectric constant (Dk) of 3.78, the antenna's performance, particularly its gain, is not much compromised despite reduction in size, compared to the standard patch antenna. Antenna configuration and miniaturization principles are discussed in Section II and Section III, respectively. Parametric analysis relevant on visa is explained in section IV.

We have investigated single SIW cavity antenna performances in section V. Section VI concludes the paper.

II. ANTENNA DESIGN

Fig.1 illustrates exploded view of the proposed antenna for 28GHz frequency band. The patch size is $1.92~\mathrm{mm}\,(w_p) \times 1.92~\mathrm{mm}\,(l_p)$ and the total area of antenna is 6 mm $(w_s) \times 6~\mathrm{mm}\,(l_s)$. The suggested antenna includes three metal layers; patch antenna on top, ground plane in the middle, and feedlines on the bottom layer. Two fused silica substrates will be bonded to server as antenna and feedline substrates with the thicknesses of 0.3mm and 0.1mm respectively. As shown in Fig. 1, meanderline (ML) is diagonally etched on the square patch antenna. This ML structure increases the electrical length, as well as the effective inductance and capacitance of a microstrip patch antenna, resulting in lower resonance frequency [12]. The proposed antenna is excited through the via feeding and a microstrip feed line on the bottom substrate in Fig. 1(b).

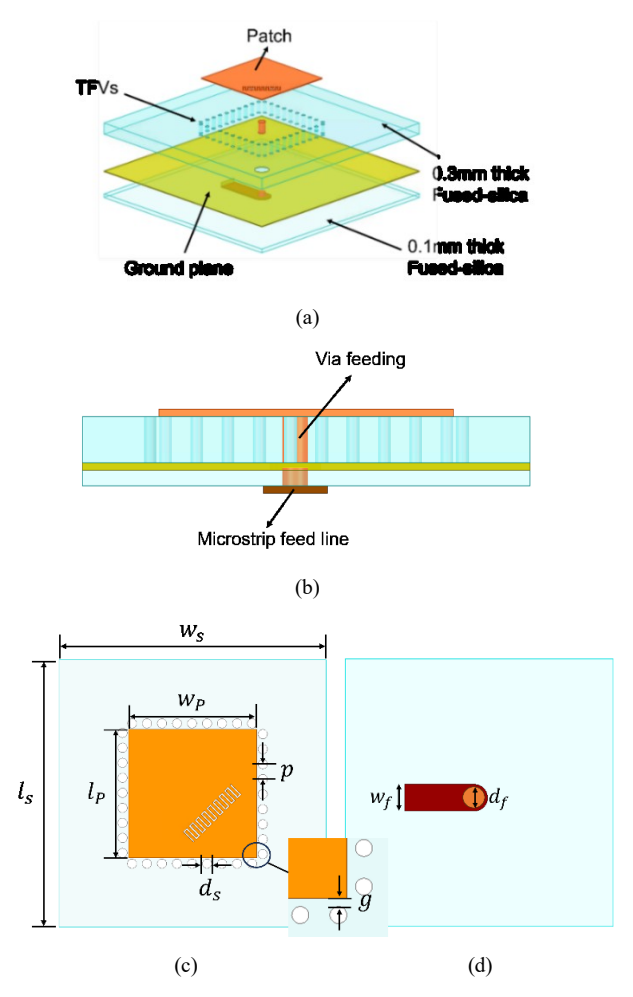


Fig. 1. Sketch of SIW cavity patch antenna on dual layer Fused-silica structure. (a) 3-D view. (b) side view. (c) top view. (d) bottom view. (w_s = 6 mm, l_s = 6 mm, w_p = 1.92 mm, l_p = 1.92 mm, p = 0.225 mm, d_s = 0.1 mm, w_f = 0.55 mm, d_f = 0.16 mm, g = 0.02 mm)

The SIW cavity wall is formed inside only the top fusedsilica substrate (0.3mm). The consists of four rows of metal vias positioned outside the patch antenna, forming the cavity sidewalls. The via diameter, d_S , and the center-to-center via pitch, p, is chosen so to meet the specific criteria of $d_S/p > 0.5$ and $d_S/\lambda_0 < 0.1$ where λ_0 is the free space wavelength. This is crucial to achieve equivalent performance compared with a conventional metallic cavity by minimizing energy leakage through spaces between vias [14]. To ensure a proper impedance matching, the diameter of the via feeding $d_f = 0.16$ mm, the width of the microstrip feed line $w_f = 0.55$ mm, via diameter $d_S = 0.5$ mm, pitches between vias p = 0.22 mm and gap between antenna and vias g = 0.02 mm are selected. Full-wave structure simulation was conducted using a high frequency structure simulator (HFSS, ANSYS Inc.) for antenna design and performance analysis.

III. MINIATURIZATION PRINCIPLE

A. Meander Line Slot

The initial miniaturization can be accomplished by adding diagonal ML-slot resonators onto the patch antenna, as shown in Fig. 2(b). The simulation results depict the electrical current distribution for both a conventional patch antenna and a patch antenna with ML-slots positioned diagonally. In the typical patch antenna, the current predominantly follows paths along the four edges of the rectangular patch. Notably, in the case of the ML-slot loaded patch antenna, a significant portion of the current is confined around the ML-slot, effectively increasing the electrical length of the patch antenna and consequently reducing its physical dimension.

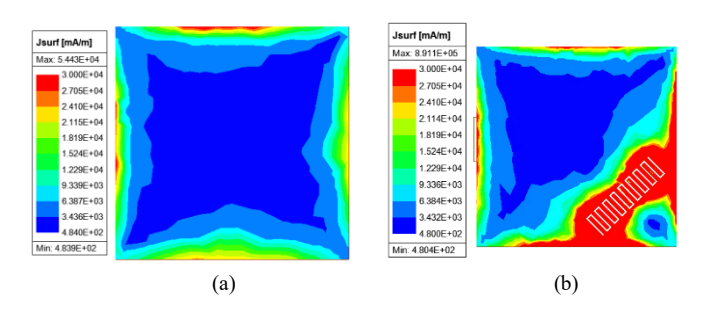


Fig. 2. Simulated current distribution on the patch antenna for the operation frequency of 28GHz. (a) normal patch antenna. (b) ML slot loaded patch antenna.

B. SIW Cavity

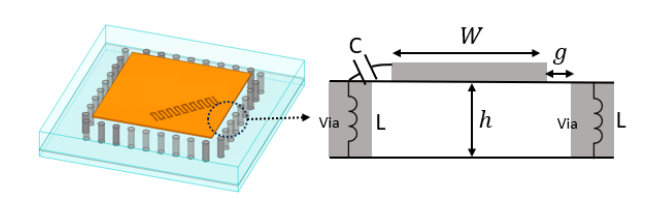


Fig. 3. SIW cavity antenna with lumped LC model

To achieve further miniaturization, the antenna is enclosed by four metalized vias positioned on the visinity of the four antenna edges, thus shaping a cavity wall as depicted in Fig. 3. The presence of the via-wall structure surrounding the patch antenna loaded with ML slot introduces additional capacitance and inductance into the antenna circuit. The capacitance \mathcal{C} from the gap between the antenna and the metalized via, and the inductance L due to the electric current flowing through the via as shown in Fig. 3, will increase the total capacitor and inductor of the patch antenna, lowering the resonance frequency baed on the equations below

$$f_r = \frac{1}{2\pi\sqrt{LC}}\tag{1}$$

$$C = \frac{W\epsilon_0(1+\epsilon_r)}{\pi} \cos h^{-1} \left(\frac{w+g}{g}\right) \tag{2}$$

$$L = \mu_0 h \tag{3}$$

where C, L, and f_r are the capacitance, inductance, and resonant frequency of a patch antenna respectively.

In this specific design, via wall can be seen as a periodic capacitors loaded on the antenna. With this capacitive loading loading, the antenna is actally a resonator based on slow-wave transmission line. Capacitive loading is proven to be an effective method to miniturize passive microwave circuits [15,16].

In Fig. 4, simulated reflection coefficient (S11) are plotted to compare the sizes of antennas with different dimensions operating at the same frequency of 28 GHz. It is observed that among them, Antenna3 possesses a more compact size, thereby demonstrating the feasibility of miniaturizing the antenna.

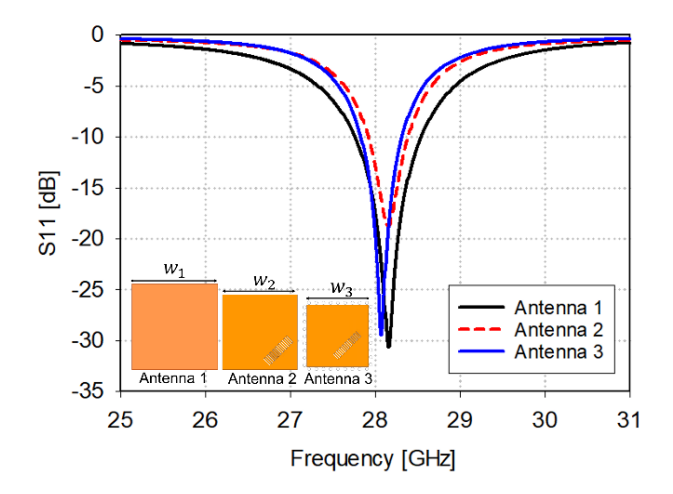


Fig. 4. Simulated return loss using three different antenna types. ($w_1 = 2.57$ mm, $w_2 = 2.3$ mm, $w_3 = 1.92$ mm)

C. 2×1 Array

The adoption of side vias in the form of a cavity encompassing the antenna will also decrease the mutual couplings in an array of antennas. (we should explain more)

To investigate the decoupling effect of the SIW cavity on a patch array, a 2×1 SIW cavity array antenna, illustrated in Fig. 5, is analyzed. Two patch antennas are placed closely, with the edge-to-edge distance, d=0.14 mm (0.026 λ_a) on a 8.06 mm × 6 mm

($w_{a1} \times l_{a1}$) on the same dual layer fused silica structure. A row of metal vias positioned at the center between the two patch antennas serves to reduce the mutual coupling factor and provide electromagnetic (EM) shielding between elements to confine EM waves within a substrate.

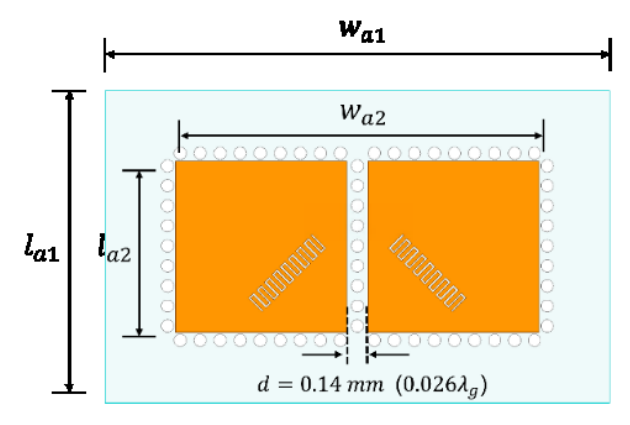


Fig. 5. Configuration of the 2 \times 1 SIW cavity array antenna on dual layer fused-silica substrate. ($w_{a1}=8.06$ mm, $l_{a1}=6$ mm, $w_{a2}=3.98$ mm, $l_{a2}=1.92$ mm, d=0.14mm)

Fig. 6 illustrates the simulation results of S11 and S12 for the 2×1 array, comparing insertion loss (S12) improvement with and without the SIW cavity. Both types of different arrays designed for operation at 28GHz exhibit resonant frequency shifts of up to 29.09 GHz, likely due to the slight coupling resulting from their close proximity. A return loss 28.62 dB and an mutual coupling -24.43 dB (S21) at 29.09 GHz. However, the array antenna without SIW cavity exhibits -8 dB mutual coupling (S21) at same frequency of 29.09 GHz. From the plotted S Parameters, it is evident that the isolation between adjacent patches improves by a maximum of 17.1 dB without the need for any additional decoupling structures, which would otherwise occupy significant space within the array configuration.

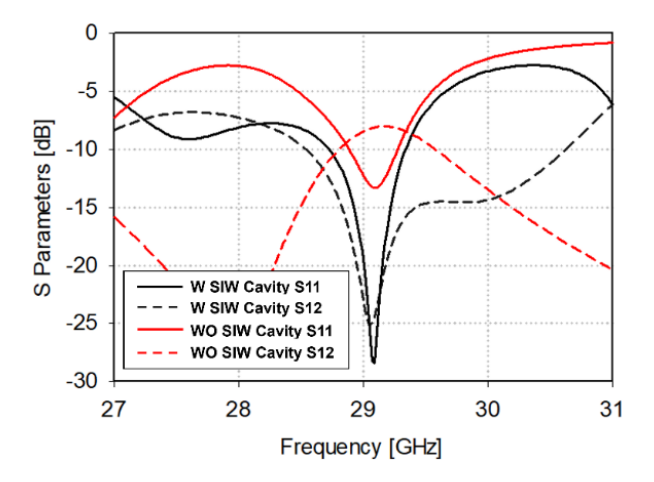


Fig. 6. Simulated S11 and S12 of the 2×1 array antenna with and without SIW cavity.

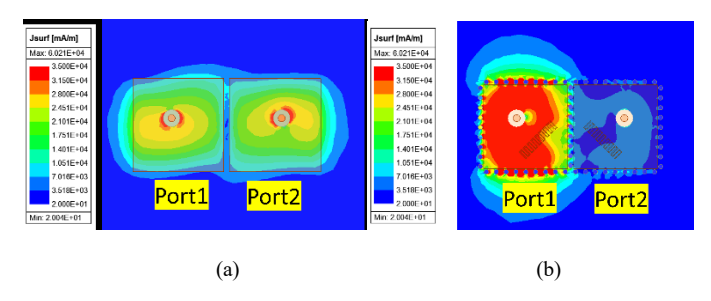


Fig. 7. Simulated surface current distribution of the 2 × 1 array antenna (a) wihout SIW cavity and (b) with SIW cavity at 29.09 GHz.

Fig. 7 represents the simulated surface current distribution for the 2 × 1 array antenna, both with and without the SIW cavity. The simulation was configured to excite only port 1 of the array, while port 2 is terminated with 50 ohm. In the antenna array without via-wall structure in Fig. 6(a), the current density appears in both patches due to mutual coupling between the two patches. However, in the SIW cavity antenna array configuration in Fig. 6(b), the via-wall between the patch antennas blocks the surface waves path from one patch to another. As the result, the Electromagnetic filed is confined only on the excited antenna.

IV. ANTENNA FREQUENCY AND IMPEDANCE MANIPULATION

In this section, we have conducted three parametric analysis to optimize the and study the effect of via size and spacing on the antenna characteristics, including return loss, impedance matching, and resonant frequency.

From Fig. 8, it is noted that gap parameter g has an impact on both input impedance and resonance frequency. As g increases, the resonance frequency shifts towards a higher value, and the input impedance approaches 50 ohm. This behavior is attributed to the change in the coupling between the metallic via and the patch antenna as the gap size varies. When the gap is smaller, the coupling is stronger, which can lead to lower input impedance, while larger gap weakens coupling, resulting in a higher input impedance. This phenomenon demonstrates that the via gap can be effectively used as a parameter to adjust the impedance of the SIW cavity antenna.

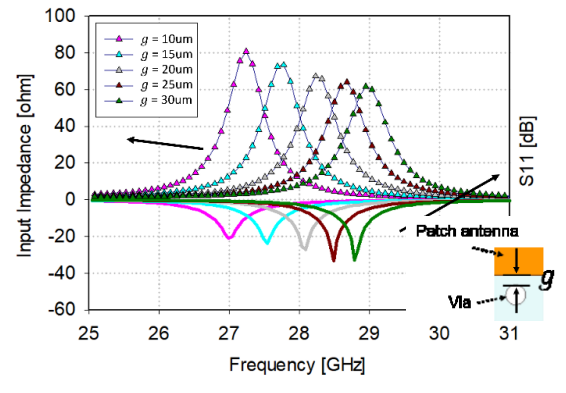
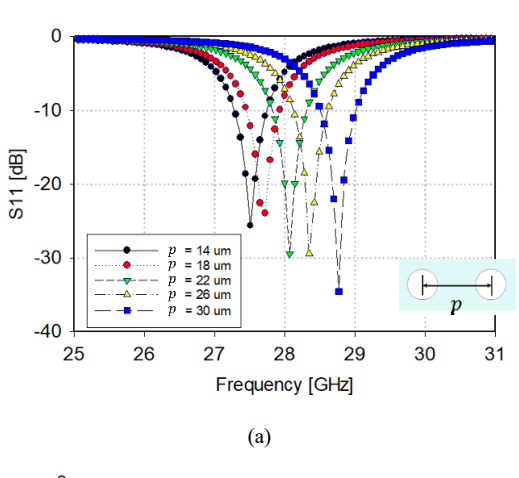


Fig. 8. Input impedance and return loss in the proposed SIW cavity antenna. The solid lines represente the return loss (S11) and lines with triangle symbol represent the input impedance.

Fig 9 indicates the simulation results of the return loss (S11) for the effects of parameters p and d_S . As the pitch p which is the distance between the center positions of two adjacent via holes decreases (smaller p), more vias are incorporated into the wall. This denser arrangement can change the electromagnetic properties of the structure, leading to a shift of the resonance frequency towards the lower as shown in Fig. 9(a). It is expected that this frequency shift is attributed to the increased capacitance and inductance introduced by the additional vias, which change the impedance of the structure and thus result in changes to the center frequency. Fig. 9(b) shows that the via diameter (d_s) does not notably influence either the return loss or the resonant frequency, except for instances where d_s is either 30 μm and 80 μm, while shows slight resonant frequency shifts. Therefore, the suggested patch antenna can be engineered by systematically modified the dimensions of the via diameter (d_s) and position of the via gap (g).



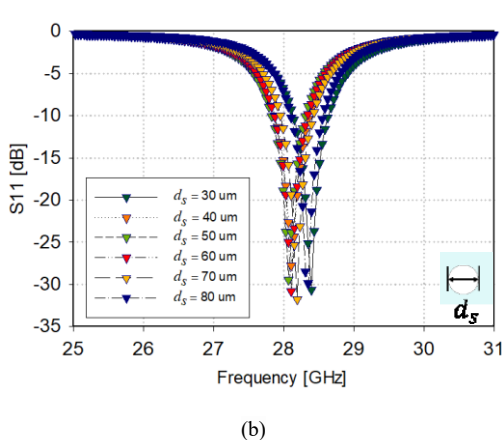


Fig. 9. Simulated S11 for the various dimentions of (a) pitch p and (b) via diameters d_S .

V. SIW CAVITY ANTENNA PERFORMANCES

Fig. 10 explains simulated radiation pattern of the proposed single SIW cavity antenna. The peak gain of this SIW cavity is 5.91 dB and the radiation efficiency is 88% at 28.08GHz. As shown in Fig. 10 (b), the symmetrical radiation pattern observed from both the xz-and yz-planes implies that the antenna has consistent radiation characteristics. Fig. 11 indicates the radiation patterns and gain of the 2×1 array antenna in the xz-and yz-plane both with and without the SIW cavity, at a

frequency of 29.09GHz. For the xz-plane in Fig. 11(a), the half-power beam width (HPBW) is 122.27° (-51.36° to 70.91°) for the standard 2×1 array antenna and 150.01° (-67.15° to 82.86°) for the 2×1 SIW cavity array antenna. In the yz -plane (Fig. 11(b)), the half-power beam width (HPBW) is 225.38° (-119.61° to 105.71°) without the SIW cavity and 255.56° (-154.98° to 100.58°) with the SIW cavity. These results demonstrate the effectiveness of the SIW cavity structure in reducing unwanted mutual coupling, resulting in improvements of 27.74° (from 122.27° to 150.01°) in the xz-plane and 30.18° (from 225.38° to 255.56°) in the yz-plane.

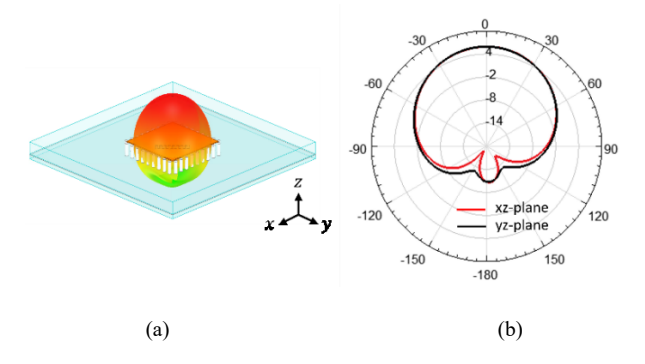


Fig. 10. Simulated (a) 3D and (b) 2D radiation pattern on single SIW cavity antenna at 28.08 GHz.

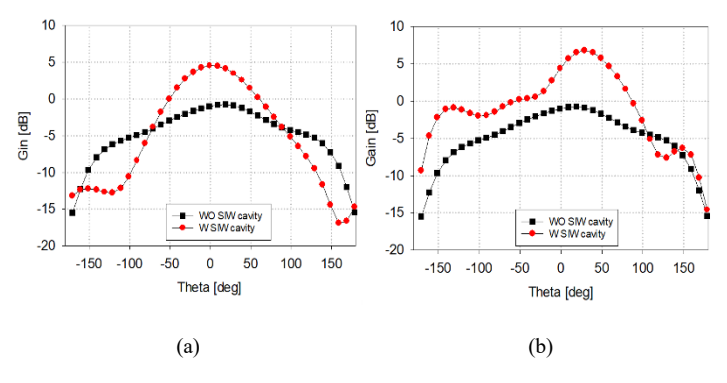


Fig. 11. Simulated radiation pattern of the 2×1 patch antenna with/without the SIW cavity in (a) xz-plane and (b) yz-plane.

Conclusion

In this paper, the novel SIW antenna is designed using TFV technology for miniaturization purposes without compromising antenna performances. The formation of a TFV-based cavity wall reduces the center frequency of the SIW antenna by creating additional equivalent capacitances. These capacitances are generated between the four rows of metallized via holes, which are situated along the outer edges of the square patch antenna, and the metallic patch antenna. In the 2x1 array configuration, mutual coupling can be greatly mitigated with a small distance (edge-to-edge) of 0.14 mm (0.026 λ_g) and isolation improvement of 17.03 dB.

VI. ACKNOWLEDGEMENTS

This material is based upon work supported by the National Science Foundation under Grant Number 2030122. The design and simulation have been performed in the University of Florida.

REFERENCES

- [1] Y. Niu, Y. Li, D. Jin, L. Su and A. V. Vasilakos, "A survey of millimeter wave communications (mmWave) for 5G: Opportunities and challenges", *Wireles Netw.*, vol. 21, no. 8, pp. 2657-2676, Nov. 2015.
- [2] R. T. Prabu, M. Benisha, V. T. Bai and V. Yokesh, "Millimeter wave for 5G mobile communication application", Int. Conf. Adv. Electr. Electron. Information Commun. Bio-Informatics, pp. 1-5, 2016.
- [3] S. Rajagopal, S. Abu-Surra, Z. Pi and F. Khan, "Antenna array design for multi-gbps mmwave mobile broadband communication", *Proc. Global Telecommun. Conf. (Globecom)*, pp. 1-6, 2011.
- [4] M. Yang, Z. N. Chen, P. Y. Lau, X. Qing and X. Yin, "Miniaturized patch antenna with grounded strips", *IEEE Trans. Antennas Propag.*, vol. 63, no. 2, pp. 843-848, 2015.
- [5] A. Boukarkar, X. Q. Lin, Y. Jiang and Y. Q. Yu, "Miniaturized Single-Feed Multiband Patch Antennas," in *IEEE Trans. Antennas Propag.*, vol. 65, no. 2, pp. 850-854, 2017.
- [6] L. Wang, X. -X. Yang, T. Lou and S. Gao, "A Miniaturized Differentially Fed Patch Antenna Based on Capacitive Slots," in *IEEE Antennas Wirel. Propag. Lett*, vol. 21, no. 7, pp. 1472-1476, 2022
- [7] Y. Dong, H. Toyao and T. Itoh, "Compact Circularly-Polarized Patch Antenna Loaded With Metamaterial Structures," in *IEEE Trans.* Antennas Propag., vol. 59, no. 11, pp. 4329-4333, 2011.
- [8] X. Y. Liu, Z. T. Wu, Y. Fan and E. M. Tentzeris, "A Miniaturized CSRR Loaded Wide-Beamwidth Circularly Polarized Implantable Antenna for Subcutaneous Real-Time Glucose Monitoring," in *IEEE Antennas Wirel*. *Propag. Lett*, vol. 16, pp. 577-580, 2017.
- [9] G. P. Mishra and B. B. Mangaraj, "Miniaturised microstrip patch design based on highly capacitive defected ground structure with fractal boundary for X-band microwave communications", *Microw. Antennas Propag.*, vol. 13, no. 10, pp. 1593-1601, 2019.
- [10] Z. Shao and Y. Zhang, "A single-layer miniaturized patch antenna based on coupled microstrips", *IEEE Antennas Wireless Propag. Lett.*, vol. 20, no. 5, pp. 823-827, 2021.
- [11] L. Wang, X. -X. Yang, T. Lou and S. Gao, "A Miniaturized Differentially Fed Patch Antenna Based on Capacitive Slots," in *IEEE Antennas Wirel. Propag. Lett*, vol. 21, no. 7, pp. 1472-1476, 2022.
- [12] H. Jang, P. Pahlavan and Y. -K. Yoon, "Highly Compact and High Gain 2 x 2 Patch Array Antenna with Slotted Meanderline Loading," *IEEE* 73rd ECTC, pp. 1917-1920, 2023
- [13] P. Pahlavan, S. -I. Choi, A. Wilcher, H. -I. Kim, H. Jang and Y. -K. Yoon, "Metamaterial Based Compact Patch Antenna Array for Antennain- Package Solutions in Frequency Handover Applications," 2023 IEEE 73rd Electronic Components and Technology Conference (ECTC), Orlando, FL, USA, 2023, pp. 475-480, doi: 10.1109/ECTC51909.2023.00085
- [14] D. Sievenpiper, "High-Impedance Electromagnetic Surfaces," Ph.D. dissertation, Dept. Elect. Eng. Univ. California at Los Angeles, Los Angeles, CA, 1999
- [15] P. Pahlavan, S. Z. Aslam and N. Ebrahimi, "A Novel Dual-band and Bidirectional Nonlinear RFID Transponder Circuitry," 2022 IEEE/MTT-S International Microwave Symposium - IMS 2022, Denver, CO, USA, 2022, pp. 44-47, doi: 10.1109/IMS37962.2022.9865478
- [16] Pahlavan, Payman, and Najme Ebrahimi. "Dual-band Harmonic and Subharmonic Frequency Generation Circuitry for Joint Communication and Localization Applications Under Severe Multipath Environment." arXiv preprint arXiv:2110.15363 (2021).